Journal of Biomolecular NMR, 1 (1991) 391–402
ESCOM

J-Bio NMR 034

Effects of internal motions on the development of the two-dimensional transferred nuclear Overhauser effect

A. Patricia Campbell and Brian D. Sykes

MRC Group in Protein Structure and Function, Department of Biochemistry, University of Alberta, Edmonton, Alberta, Canada T6G 2H7

Dedicated to the memory of Professor V.F. Bystrov

Received 10 June 1991
Accepted 16 July 1991

Keywords: Transferred nuclear Overhauser effect; NMR; Internal motions; Structure determination; Spin diffusion

SUMMARY

In this paper we address the influence of internal motions on the development of the transferred nuclear Overhauser effect in a ligand undergoing chemical exchange between a free and a bound state. We examine the effects of varying the effective correlation time as well as the motional order parameter for methyl group and phenyl ring rotations in the free and bound ligand conformations. The effect of decreasing the motional order for a proton pair on a methyl group or phenyl ring is to decrease the effective correlation time of the internuclear vector, and thus to decrease the cross-relaxation rate between the proton pair. This functions to dampen the effects of spin diffusion, especially in the bound ligand where cross-relaxation rates are much faster than in the free ligand. The effect of changing the effective correlation time for methyl group motions has little effect on the build-up behaviour of the transferred nuclear Overhauser effect for small values of fraction bound, but a larger effect on how fast it decays. This effect is greater for internal motions in the free peptide than it is for internal motions in the bound peptide.

INTRODUCTION

One of the most important issues in biology is the interaction of ligands with macromolecules. Examples include the interaction of substrates with enzymes, antigens with antibodies, hormones with receptors, nucleotides with regulatory proteins, and peptides with phospholipids. Excepting those instances where the ligand has been crystallized in a complex with the macromolecule, nuclear magnetic resonance spectroscopy (NMR) provides the best techniques for the determination of the structure of the bound ligand. Concomittant with the rapid developments in two-dimensio-

Abbreviations: NMR, nuclear magnetic resonance; NOE, nuclear Overhauser enhancement; TRNOE, transferred nuclear Overhauser enhancement; TRNOESY, two-dimensional transferred nuclear Overhauser enhancement spectroscopy; TnC, troponin C; TnI, troponin I.

0925-2738/$ 5.00

nal NMR techniques and the use of NMR to determine the structure of proteins in solution (Wüthrich, 1986), there has been a recent emergence of interest in the transferred nuclear Overhauser enhancement experiment originally proposed by Balaram and Bothner-By (1972a,b). This is evidenced by the large number of bound ligand structures that have been investigated using the TRNOE within the past five years (Banerjee et al., 1985; Ehrlich and Colman, 1985,1990; Ferrin and Mildvan, 1985; Clore et al., 1986; Glasel and Borer, 1986; Anderson et al., 1987; Ito et al., 1987; Meyer et al., 1988; Anglister et al., 1989; Glasel, 1989; Levy et al., 1989; Ni et al., 1989a,b,c,1990; Anglister and Zilber, 1990; Bevilacqua et al., 1990; Milon et al., 1990).

The TRNOE is the extension of the two-dimensional nuclear Overhauser effect to exchanging systems such as ligand–protein complexes. The intramolecular TRNOE allows the transfer of information concerning cross-relaxation between two nuclei in the bound ligand to the free ligand resonances via chemical exchange. Recently Landy and Rao (1989) have developed a full relaxation matrix analysis for the TRNOE, analogous to the full relaxation matrix treatment of NOE data which has been used to refine many protein and nucleic acid structures (Keepers and James, 1984; Lefevre et al., 1987; Boelens et al., 1988; Borgias and James, 1988,1989; Baleja et al., 1990).

We have recently published a theoretical evaluation of the TRNOE using the full relaxation matrix approach (Campbell and Sykes, 1991a). We examined the effects of variables such as mixing time, fraction of bound peptide, free and bound correlation times, and other contributions to spin-lattice relaxation rates in an attempt to offer practical experimental guidelines for the design of a TRNOE experiment. These studies, however, did not fully address the question of internal motions in the free and bound peptide, and how these internal motions affect the development of the TRNOE. In this paper we address the influence of internal motions on the TRNOE, and issues that are introduced into the calculations such as chemically equivalent protons and the scaling of TRNOE cross-peak intensities (Yip, 1990).

THEORY

A description of homonuclear dipolar relaxation for a multiple spin system requires the complete set of coupled differential equations describing the evolution of longitudinal magnetization of the individual spins (Bloch, 1957). These coupled differential equations can be written in matrix form (Solomon, 1955; Abragam, 1961; Macura and Ernst, 1980)

$$d\mathbf{M}/d\tau_m = -\mathbf{W}\cdot\mathbf{M} \tag{1}$$

where $\mathbf{M}$ is the vector of magnetization and $\mathbf{W}$ is the n-dimensional relaxation matrix. Equation 1 can be solved as (Bull, 1987)

$$\mathbf{M}(\tau_m) = \exp(-\mathbf{W}\tau_m)\,\mathbf{M}(0) = \chi\,\exp(-\lambda\tau_m)\,\chi^{-1}\,\mathbf{M}(0) = \mathbf{a}(\tau_m)\,\mathbf{M}(0) \tag{2}$$

where χ is the matrix of eigenvectors of the relaxation matrix $\mathbf{W}$, λ is the diagonal matrix of eigenvalues, and $\mathbf{a}$ is the matrix of mixing coefficients which are proportional to the measured NOE intensities.

If the spin system undergoes chemical exchange between a free (F) and bound state (B), relaxation can be described by

$$\frac{d}{d\tau_m}\begin{bmatrix}\mathbf{m_B}\\ \mathbf{m_F}\end{bmatrix} = -\mathbf{R}\begin{bmatrix}\mathbf{m_B}\\ \mathbf{m_F}\end{bmatrix} \tag{3}$$

where $\mathbf{m_B}$ and $\mathbf{m_F}$ are n-dimensional vectors, $\mathbf{R} = \mathbf{E} + \mathbf{W}$, where $\mathbf{E}$ is the chemical exchange matrix, and $\mathbf{W}$ is the 2n-dimensional relaxation matrix for the n-spin system in the free and bound forms (Landy and Rao, 1989).

To obtain the mixing coefficients $a_{ij}(\tau_m)$, $\mathbf{R}$ must be diagonalized to yield λ, the eigenvalue matrix. But due to the lack of symmetry in matrix $\mathbf{R}$, computer methods for the diagonalization are not so readily available and the eigenvalues are not guaranteed to be real (Landy and Rao, 1989). These complications may be avoided in the regime of fast chemical exchange. In the limit of fast chemical exchange, the longitudinal magnetization of the spin system, summed over the exchanging species, decays as a function of the population-weighted average of the individual relaxation matrices for the bound and free states (Landy and Rao, 1989)

$$\frac{d(\mathbf{m_B}+\mathbf{m_F})}{d\tau_m} \cong (p_B\mathbf{W_B} + p_F\mathbf{W_F})\,(\mathbf{m_B}+\mathbf{m_F}) \tag{4}$$

where $\mathbf{W_B}$ and $\mathbf{W_F}$ are relaxation matrices for the bound and free states respectively, and p_B and p_F are the fractions of bound and free ligand.

Calculating the average relaxation matrix, $\mathbf{R} \cong p_B\mathbf{W_B} + p_F\mathbf{W_F}$, requires setting up individual relaxation matrices, $\mathbf{W_B}$ and $\mathbf{W_F}$. Each relaxation matrix is set up identically, in the following manner. Equation 1 may then be represented as

$$\frac{d}{d\tau_m}\begin{bmatrix} m_i \\ m_j \\ \vdots \\ m_n \end{bmatrix} = -\begin{bmatrix} W_{ii} & W_{ji} & \cdots & W_{in} \\ W_{ji} & W_{jj} & \cdots & W_{jn} \\ & \vdots & & \\ W_{ni} & W_{nj} & \cdots & W_{nn} \end{bmatrix}\begin{bmatrix} m_i \\ m_j \\ \vdots \\ m_n \end{bmatrix} \tag{5}$$

where the diagonal elements are given by

$$W_{ii} = 2(m_{oi} - 1)\,(W_{1ii} + W_{2ii}) + \sum_k m_{ok}\,(W_{0ik} + 2W_{1ik} + W_{2ik}) + R_{1ext} \tag{6a}$$

and the off-diagonal elements are given by

$$W_{ij} = m_{oi}(W_{2ij} - W_{0ij}) \tag{6b}$$

To take into account other possible relaxation pathways we have added an external relaxation component, R_{1ext}, to the diagonal element, W_{ii}. The transition probabilities are given by (Macura and Ernst, 1980)

$$W_{1ii} = 3/2\; q_{ii}\; J(\omega_i) \tag{7a}$$

$$W_{2ii} = 6\; q_{ii}\; J(2\omega_i) \tag{7b}$$

$$W_{1ij} = 3/2\ q_{ij}\ J(\omega_i) \tag{7c}$$

$$W_{0ij} = q_{ij}\ J(\omega_i - \omega_j) \tag{7d}$$

$$W_{2ij} = q_{ij}\ J(\omega_i + \omega_j) \tag{7e}$$

Here the spectral density functions take the form

$$J(\omega_i) = \tau_c/(1 + (\omega_i \tau_c)^2) \tag{8}$$

and

$$q_{ij} = 1/10\ \gamma_i^2\ \gamma_j^2\ h^2\ (r_{ij})^{-6}\ (\mu_0/4\pi) \tag{9}$$

where τ_c is the overall tumbling time of the peptide which modulates the interaction between spins i and j, and r_{ij} is the internuclear distance.

Chemically equivalent protons

The off-diagonal elements, W_{ij} and W_{ji}, are equivalent only if we ignore the presence of chemically equivalent groups of protons for which $m_{oi} > 1$, such as methyl groups or aromatic rings in the presence of fast internal motion. This results in an asymmetric relaxation matrix for which the eigenvalues are not guaranteed to be real. In addition, most computer algorithms for diagonalizing relaxation matrices are available for symmetric matrices only (Borgias and James, 1988,1989). When the relaxation matrix, **W**, is real and symmetric, then the transformation matrix of orthonormal eigenvectors, χ, is a unitary matrix which has the mathematical property of having its inverse equal to its transpose ($\chi^{-1} = \chi^T$). Thus, Eq. 2 simplifies to

$$\mathbf{M}(\tau_m) = \chi \exp(-\lambda \tau_m) \chi^T \mathbf{M}(0) \tag{10}$$

The computer algorithm required to calculate the transpose of a matrix (as opposed to its inverse) is much simpler and computationally faster, especially as the size of the matrix increases, and thus there are computational advantages in starting with a symmetric relaxation matrix as a starting point for relaxation matrix analysis.

We considered two choices for the treatment of groups of equivalent protons: (1) the use of a single coordinate position for a pseudo proton situated geometrically in the center of the equivalent group of protons, or (2) the explicit consideration of each proton in the group. Treating each proton as an individual distinguishable proton generates a symmetric matrix ($m_{oi} = 1$). This choice is valid as long as no second order spin coupling is involved. Under these conditions, the TRNOE between a given proton and a group of equivalent protons is the sum of the contributions from each equivalent proton in the group to the given proton. The same reasoning is involved when considering the scaling of experimental cross-peak intensities when groups of equivalent protons are involved (Yip, 1990). Cross-relaxation amongst the group of equivalent protons is calculated explicitly.

Effects of internal motion

To take into account differential motion, we incorporated the order parameters S_{iF} and S_{iB} for spin i in the free and bound peptide (Baleja et al., 1990), using Lipari's and Szabo's model free approach (Lipari and Szabo, 1982). In this approach, internal motions in macromolecules may be specified by two independent quantities: a generalized order parameter, S^2 and an effective internal correlation time τ_e. The order parameter, S^2, can vary between 0 and 1. A value of one indicates that the correlation time of the interproton vector is the same as the overall tumbling time of the peptide (τ_c); a value of zero indicates complete motional freedom.

The spectral density function of Eq. 8 then becomes

$$J(\omega_i)=[S^2\tau_c/(1+(\omega_i\tau_c)^2)]+[(1-S^2)\tau/(1+(\omega_i\tau)^2)] \tag{11}$$

where

$$1/\tau=1/\tau_c+1/\tau_e \tag{12}$$

RESULTS

Using a model system undergoing chemical exchange, we have computer-generated TRNOE build-up curves and have used these as a tool to investigate the effects of internal motion, particularly within methyl and aromatic groups. As a model system, we have chosen the binding of a 12-residue peptide, spanning the inhibitory region of the muscle protein troponin I, to the muscle protein troponin C. This system has been used in our previous calculations (Campbell and Sykes, 1989,1991a), is of general biochemical interest, and is a system for which experimental data is available. We have determined the structure of the synthetic inhibitory peptide Nα-acetyl TnI(104–115) amide bound to Ca(II)-saturated skeletal turkey TnC (Campbell and Sykes, 1989,1991b) and we will take this as the bound structure. The TRNOE-derived structure of the TnI peptide bound to TnC reveals an amphiphilic helical structure, distorted in the center by the proline residues. The central bend in the peptide functions to bring the residues on the hydrophobic face into closer proximity with each other, thereby forming a small hydrophobic pocket with the aromatic ring of Phe^{106} being somewhat buried by the side chains of Leu^{111} and Val^{114}. The hydrophilic, basic residues extend off the opposite face of the peptide. The coordinates for the free TnI peptide were generated from the standard φ,ψ angles of a β-strand ($\varphi=-118°$, $\psi=+118°$). Explicit methyl protons were added to the free and bound TnI peptide structures using a program which places protons in an sp^3-hybridized geometry about the central carbon atom.

The computer simulation takes as input the coordinates of the protons of the free and bound conformations of the TnI peptide, the overall tumbling times of the free and bound peptide (τ_{cF}, τ_{cB}), the effective internal correlation times of the free and bound peptide (τ_{eF}, τ_{eB}), the external leakage relaxation rates of the free and bound peptide protons (R_{1extF}, R_{1extB}), order parameters for individual free and bound peptide protons (S_{iF}, S_{iB}), the fraction of the free and bound peptide (p_F, p_B), the mixing time (τ_m) and the frequency of the experiment (ω). The values of the parameters are as used previously ($\tau_{cF}=0.4$ ns, $\tau_{cB}=25$ ns, $R_{1extF}=1.0\ s^{-1}$, $R_{1extB}=2.0\ s^{-1}$) (Campbell and Sykes, 1991a) to facilitate comparison. The proton coordinates of the TnC protein to which

the TnI peptide binds were not included explicitly in the calculation, but rather as a bath of protons in which the bound TnI peptide experiences a longer correlation time and a larger external leakage relaxation rate.

The specific TRNOEs studied were the intraresidue interaction between the αCH of Val^{114} and the six-chemical-shift degenerate γCH_3 protons of the same residue, and the longer range interresidue interaction between these six γCH_3 of Val^{114} and three chemical-shift degenerate protons of Phe^{106} (two εCH and one ζCH aromatic ring protons). If internal motions are important, they should be obvious in these interactions.

To estimate the values of S_{iF} and S_{iB} to use in these simulations, we considered the fact that for a methyl group rotating around a carbon-carbon single bond, τ_c should be decreased by a factor of $S^2 = ([3\cos^2\theta - 1]/2)^2$ (Marshall et al., 1972) where θ is the angle between the i-j interproton vector and the axis of rotation (the carbon-carbon single bond). For an sp^3-hybridized methyl group, $\theta = 90°$, making $S^2 = ([3\cos^2\theta - 1]/2)^2 = 0.25$ for rotation around the methyl axis. Thus, for the methyl protons i and j of the Val^{114} residue in the bound and free peptide, we have chosen $S_i{*}S_j = 0.25$, or $S_i = S_j = 0.5$. As far as aromatic rings are concerned, the geometry leads to different estimations of $S_i{*}S_j$ values for the different proton pairs of the ring, so we have somewhat arbitrarily chosen $S_i = 0.5$ for the δ, ξ and ζ aromatic protons of the Phe^{106} residue in the free and bound peptide.

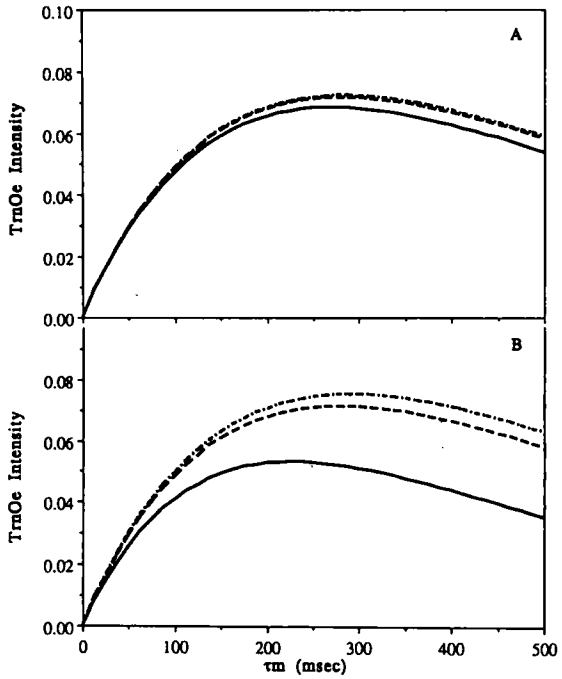

Fig. 1. TRNOE intensity versus mixing time (τ_m) for various free (τ_{eF}) and bound (τ_{eB}) internal correlation times. For panel A, $\tau_{eF} = 0.01$ ns and $S_{iF} = S_{iB} = 0.5$ for the Val^{114} methyl protons: (——) $\tau_{eB} = 0.1$ ns; (– – –) $\tau_{eB} = 0.01$ ns; (– – –) $\tau_{eB} = 0.001$ ns. For panel B, $\tau_{eB} = 0.01$ ns and $S_{iF} = S_{iB} = 0.5$ for the Val^{114} methyl protons: (——) $\tau_{eF} = 0.1$ ns; (– – –) $\tau_{eF} = 0.01$ ns; (– – –) $\tau_{eF} = 0.001$ ns. Other parameters used in the simulation were $\omega = 500 \times 10^6$ s^{-1}, $R_{1extF} = 1.00$ s^{-1}, $R_{1extB} = 2.00$ s^{-1}, $\tau_{cB} = 25$ ns, $\tau_{cF} = 0.4$ ns, $p_B = 0.1$.

Figure 1 shows the effect of varying the effective internal correlation times for methyl group motions in the free and bound peptide on the development of the TRNOE for the intraresidue $Val^{114}\alpha CH$–$(\gamma CH_3)_2$ interaction. In panel A, τ_{eF} is kept constant at 0.01 ns, whereas τ_{eB} is varied from 0.001 ns to 0.1 ns. In panel B, τ_{eB} is kept constant at 0.01 ns, whereas τ_{eF} is varied from 0.001 ns to 0.1 ns. The order parameters for individual free and bound peptide methyl protons were set at $S_{iF} = S_{iB} = 0.5$. One can see that changing the effective correlation time for methyl group motions has little effect on the build-up behaviour of the TRNOE (at the low fraction bound used), but a larger effect on how fast it decays. This effect is greater for internal motions in

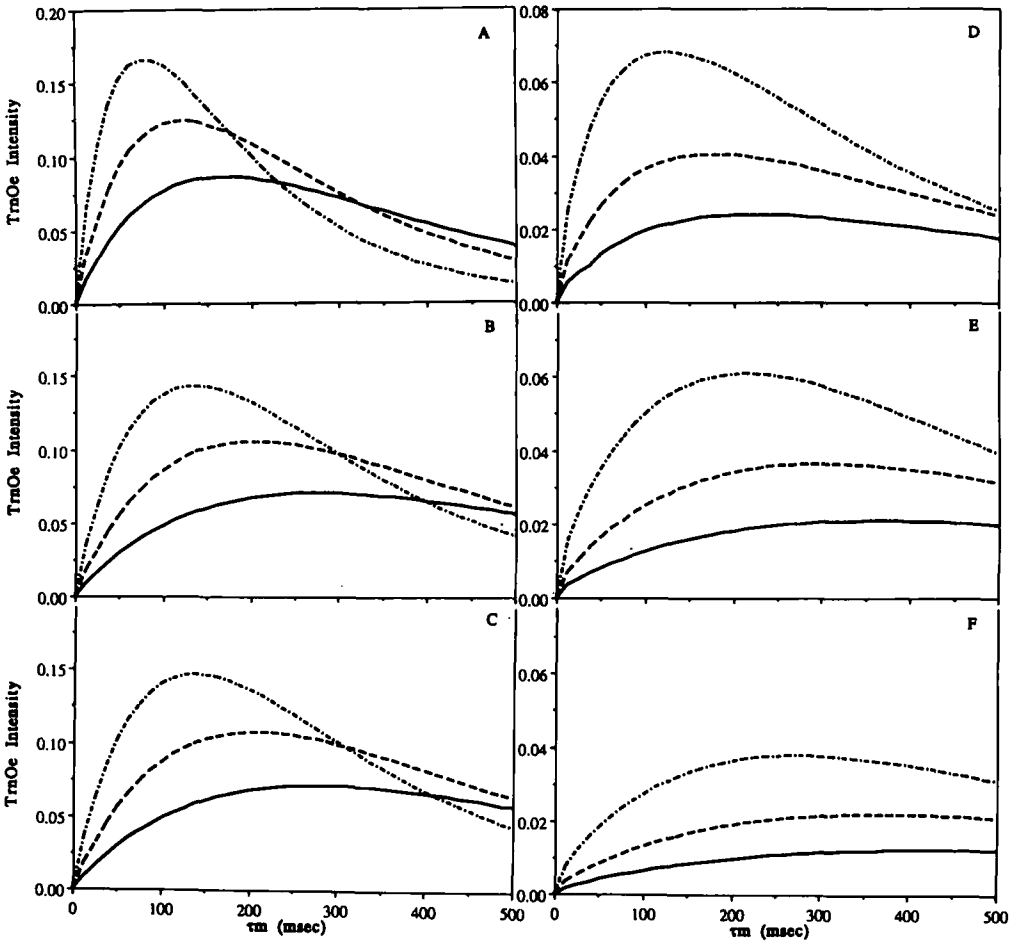

Fig. 2. TRNOE intensity versus mixing time (τ_m) for various fractions of bound peptide (p_B): (—) $p_B = 0.1$; (– – –) $p_B = 0.2$; (– · –) $p_B = 0.4$. Panels A–C represent the intraresidue $Val^{114}\alpha CH$–$(\gamma CH_3)_2$ interaction, and panels D–F represent for the interresidue $Phe^{106}(\varepsilon CH_2\zeta CH)$–$Val^{114}(\gamma CH_3)_2$ interaction. For panels A and D, $S_{iF} = S_{iB} = 1.0$ for the Val^{114} methyl protons and $S_{iF} = S_{iB} = 1.0$ for the Phe^{106} ring protons. For panels B and E, $S_{iF} = S_{iB} = 0.5$ for the Val^{114} methyl protons and $S_{iF} = S_{iB} = 1.0$ for the Phe^{106} ring protons. For panels C and F, $S_{iF} = S_{iB} = 0.5$ for the Val^{114} methyl protons and $S_{iF} = S_{iB} = 0.5$ for the Phe^{106} ring protons. Other parameters used in the simulation were $\omega = 500 \times 10^6\ s^{-1}$, $R_{1extF} = 1.00\ s^{-1}$, $R_{1extB} = 2.00\ s^{-1}$, $\tau_{cB} = 25$ ns, $\tau_{cF} = 0.4$ ns, $\tau_{eB} = 0.01$ ns, $\tau_{eF} = 0.01$ ns.

the free peptide than it is for internal motions in the bound peptide. Thus, motions in the free peptide contribute more to the overall relaxation of the exchanging system than do motions in the bound peptide, a consideration which may be easily overlooked given the emphasis on the faster cross-relaxation in the bound peptide which determines the build-up rates of the TRNOE. Looking at panel B, one can see that the less rapid the internal motion about the methyl group axis in the free peptide, the more strongly is overall relaxation affected, a function of the fact that for longer τ_e values, τ approaches the inverse of the Larmor frequency, and spin-lattice T_1 relaxation becomes more effective. We have chosen $\tau_{eF}=\tau_{eB}=0.01$ ns for the subsequent TRNOE calculations, so that they do not depend strongly on the actual rate of the internal motion.

Figure 2 shows the TRNOE build-up curves for the intraresidue Val$^{114}\alpha$CH–(γCH$_3$)$_2$ and interresidue Phe^{106}(ξCH$_2\zeta$CH)–Val^{114}(γCH$_3$)$_2$ interactions calculated in the absence of methyl or ring motions in panels A and D, in the presence of methyl rotation in panels B and E, and in the presence of both methyl and ring rotation in panels C and F. One can see that the effect of internal motion is not only to dampen the buildup of the TRNOE, but also to dampen its relaxation. The build-up behaviour of the TRNOE is effectively diminished at shorter mixing times but 'spread-out' over longer mixing times. This effect is evident for the intraresidue Val$^{114}\alpha$CH–(γCH$_3$)$_2$ interaction (Figs. 2A–C) only for the methyl rotation, but the effects of both methyl and ring motion are evident for the interresidue Phe^{106}(ξCH$_2\zeta$CH)–Val^{114}(γCH$_3$)$_2$ interaction (Figs. 2D–F). Examining the intraresidue Val$^{114}\alpha$CH – (γCH$_3$)$_2$ interaction first we can see that Figs. 2B and 2C are virtually identical, the only difference being that in Fig. 2B, motion was incorporated for only the methyl groups, whereas in Fig. 2C, motion was incorporated for both the methyl and the ring groups in the peptide. However, for the interresidue Phe^{106}(ξCH$_2\zeta$CH)–Val^{114}(γCH$_3$)$_2$ interaction, we can see that Figs. 2E and F are quite different due to the incorporation of ring motion absent for Fig. 2E but present for Fig. 2F.

In Fig. 3 (A–E) the two sets of calculations presented in Fig. 2 are converted to apparent distances that would be calculated for these interactions by using a reference TRNOE calculated at the same fraction bound and mixing time; $r_{app}=r_{ref}\ \{[(TRNOE)_{ref}(m_{oi}\cdot m_{oj})_{obs}]/[(TRNOE)_{obs}(m_{oi}\cdot m_{oj})_{ref}]\}^{1/6}$ (Yip, 1990). As a reference proton pair we have chosen the adjacent δCH-ξCH protons on the aromatic ring of Phe^{106} for which a reference TRNOE was calculated and a reference distance of 2.48 Å (invariant of secondary peptide conformation) was measured. This reference proton pair has been used in previous calculations (Campbell and Sykes, 1991a). For comparison, the actual calculated distance summed and averaged over the protons involved

$$\frac{1}{r_{av}}=\left[\frac{1}{(m_{oi}+m_{oj})}\right]\sum_{i,j}\left[\frac{1}{r_{ij}^6}\right]^{1/6} \tag{13}$$

is 2.80 Å for the intraresidue Val$^{114}\alpha$CH–(γCH$_3$)$_2$ interaction, and 3.74 Å for the interresidue Phe^{106}(εCH$_2\zeta$CH)–Val^{114}(γCH$_3$)$_2$ interaction. All distances were measured from the coordinates of the TnI peptide bound to TnC (Campbell and Sykes, 1991b). The fact that the internal motion of the phenylalanine ring influences the reference TRNOE is evidenced by the change in apparent distance observed between Figs. 3B and C for the intraresidue Val$^{114}\alpha$CH–(γCH$_3$)$_2$ interaction, for which the TRNOE build-up curves (Figs. 2B and C) are virtually identical.

We begin first with a discussion of the effects of internal motion on the calculated distance, r_{app},

for the intraresidue Val^{114}αCH–(γCH$_3$)$_2$ interaction (Figs. 3A–C). In the absence of both methyl and ring rotation (Fig. 3A), the calculated distance r_{app} is observed to increase from approximately 2.9 Å at $\tau_m = 0$ to larger values for $\tau_m > 0$. Thus, r_{app} starts from a value close to the actual averaged distance of 2.80 Å, but continues to increase to much larger values. This occurs as a result of spin diffusion which bleeds magnetization away from the Val^{114}αCH–(γCH$_3$)$_2$ interaction, leading to smaller TRNOE cross-peak intensities and larger calculated distances. The increase in r_{app} at longer τ_m is more pronounced for larger p_B. In the presence of methyl rotation (Fig. 3B), r_{app} is observed to decrease from approximately 3.2 Å at $\tau_m = 0$ and approach the actual calculated

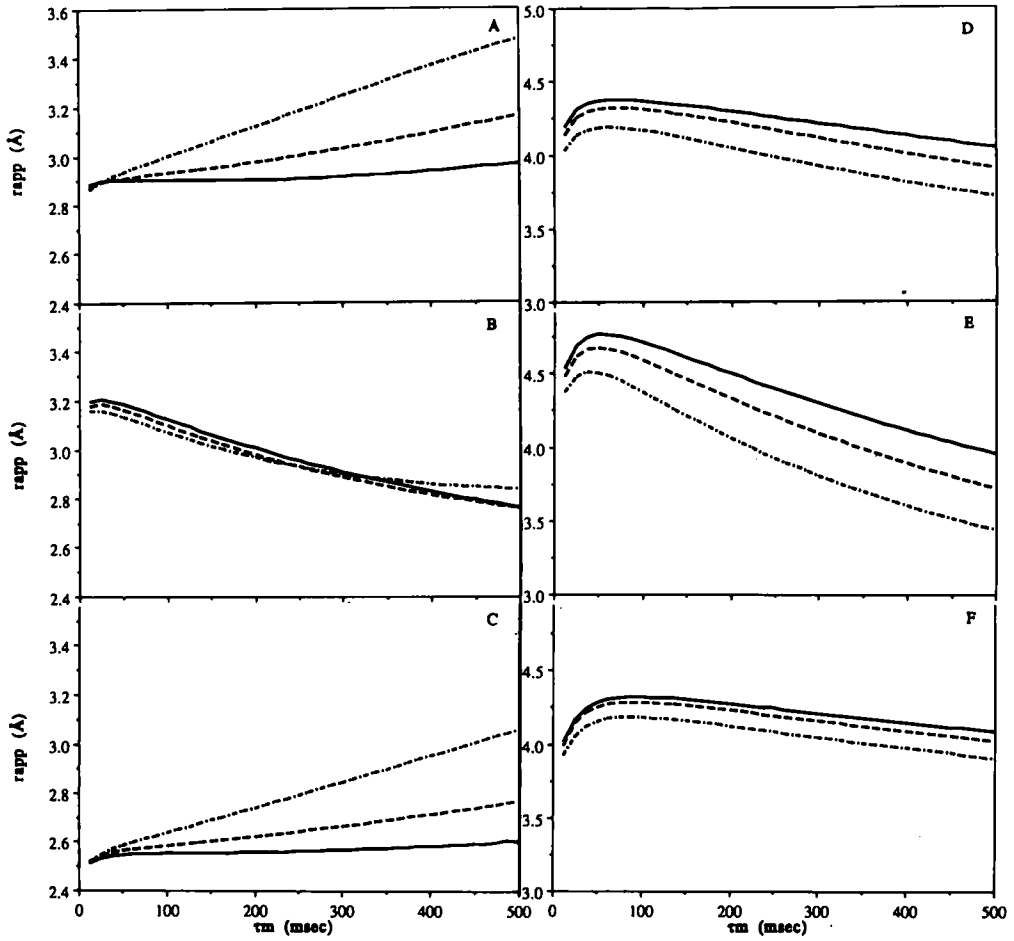

Fig. 3. r_{app} calculated from TRNOE values of Fig. 1 versus mixing time (τ_m) for various fractions of bound peptide (p_B): (——) $p_B = 0.1$; (– – –) $p_B = 0.2$; (– · –) $p_B = 0.4$. Distances were calculated using F106δCH-F106εCH as the reference TRNOE intensity and reference distance, 2.48 Å. Panels A–C represent the intraresidue Val^{114}αCH–(γCH$_3$)$_2$ interaction, and panels D–F represent for the interresidue Phe^{106}(εCH$_2$ζCH)–Val^{114}(γCH$_3$)$_2$ interaction. For panels A and D, $S_{iF} = S_{iB} = 1.0$ for the Val^{114} methyl protons and $S_{iF} = S_{iB} = 1.0$ for the Phe^{106} ring protons. For panels B and E, $S_{iF} = S_{iB} = 0.5$ for the Val^{114} methyl protons and $S_{iF} = S_{iB} = 1.0$ for the Phe^{106} ring protons. For panels C and F, $S_{iF} = S_{iB} = 1.0$ for the Val^{114} methyl protons and $S_{iF} = S_{iB} = 0.5$ for the Phe^{106} ring protons.

distance of 2.80 Å for $\tau_m > 0$. This occurs as a result of the relaxation damping effect of the internal motion which effectively diminishes the TRNOE at shorter mixing times but 'spreads-out' the TRNOE over longer mixing times. The decrease in r_{app} at longer τ_m is virtually independent of p_B as the three curves for the three values of fraction bound are almost superimposable. In the presence of both methyl and ring rotation (Fig. 3C), r_{app} is observed to increase from approximately 2.5 Å to larger values for $\tau_m > 0$, once again increasing to values much larger than the real value of 2.80 Å. The behaviour of the r_{app} versus τ_m curves is similar to the behaviour observed in the absence of either methyl or ring motion, and is strongly dependent on p_B. The effect of incorporating motion in the reference TRNOE, Phe$^{106}\delta$CH–ξCH, serves to counteract the effect of motion in the experimental TRNOE, Val$^{114}\alpha$CH–(γCH$_3$)$_2$, essentially making it appear as if the Val^{114} methyl group were static.

The effects of motion are manifested somewhat differently in the interresidue interaction, Phe^{106}(εCH$_2\zeta$CH)–Val^{114}(γCH$_3$)$_2$ (Figs. 3D–F). In the absence of both methyl and ring rotation (Fig. 3D), the calculated distance r_{app} is observed to decrease from approximately 4.0 Å at $\tau_m = 0$ and approach the actual calculated distance of 3.74 Å for $\tau_m > 0$. In the presence of methyl rotation (Fig. 3E), the decrease in r_{app} as a function of τ_m is more rapid. At $\tau_m = 0$, r_{app} is approximately 4.5 Å, but for $\tau_m > 0$ rapidly decreases to values much smaller than the actual calculated distance of 3.74 Å. From Figs. 3D and E, it can be seen that the behaviour of the r_{app} versus τ_m curves observed in the absence of ring motion is strongly dependent on p_B. In the presence of both methyl and ring rotation (Fig. 3F), r_{app} is observed to slowly decrease from approximately 4.0 Å at $\tau_m = 0$ and approach the actual averaged distance of 3.74 Å for $\tau_m > 0$. The behaviour of the r_{app} versus τ_m curves is similar to the behaviour observed in the absence of either methyl or ring motion, but is not so strongly dependent on p_B. Incorporating ring motion affects both the reference TRNOE, Phe$^{106}\delta$CH–ξCH, and the experimental TRNOE, Phe^{106}(εCH$_2\zeta$CH)–Val^{114}(γCH$_3$)$_2$. Thus, the effect of incorporating motion in the reference TRNOE does not entirely counteract the effect of motion in the experimental TRNOE, since the magnitude of the experimental TRNOE is also affected by ring motion.

It is interesting to note the difference in the behaviour of the r_{app} versus τ_m curves for the shorter-range intraresidue Val$^{114}\alpha$CH–(γCH$_3$)$_2$ interaction versus the longer-range interresidue Phe^{106}(εCH$_2\zeta$CH)–Val^{114}(γCH$_3$)$_2$ interaction. In the absence of any motion, the r_{app} for the Val$^{114}\alpha$CH–(γCH$_3$)$_2$ interaction increased with increasing τ_m (Fig. 3A), whereas the r_{app} for the Phe^{106}(εCH$_2\zeta$CH)–Val^{114}(γCH$_3$)$_2$ interaction decreased with increasing τ_m (Fig. 3D). The incorporation of motion tends to shift the curves in the opposite direction so that the r_{app} for the Val$^{114}\alpha$CH–(γCH$_3$)$_2$ interaction decreased slightly with increasing τ_m (Fig. 3B), and the r_{app} for the Phe^{106}(εCH$_2\zeta$CH)–Val^{114}(γCH$_3$)$_2$ interaction remained more or less constant for increasing τ_m (Fig. 3F). Thus, the effect of incorporating internal motions when calculating apparent distances from a set of TRNOESY intensities gathered at longer τ_m and larger p_B would be to shorten intraresidue distances and lengthen interresidue distances. The incorporation of internal motions would serve to counteract the effects of spin diffusion which make shorter intraresidue distances appear longer and longer interresidue distances appear shorter.

CONCLUSION

In this manuscript we have addressed the influence of internal motions on the development of

the TRNOE in a ligand undergoing chemical exchange between a free and a bound state. The effect of adding internal motion within a proton pair on the ligand is to decrease the correlation time of the internuclear vector, and thus to decrease the cross-relaxation rate between the proton pair. This functions to dampen the effects of spin diffusion, especially in the bound ligand where cross-relaxation rates are much faster than in the free ligand. The build-up behaviour of the TRNOE is effectively diminished at shorter mixing times but 'spread-out' over longer mixing times. However, for small values of fraction bound, and at short mixing times where the TRNOE build-up curves are linear, the effects of internal motion (like the effects of spin diffusion) are not that noticeable, and the apparent distances approach the calculated average distances in the bound ligand. Changing the effective correlation time for methyl group motions has little effect on the build-up behaviour of the TRNOE for small values of fraction bound, but a larger effect on how fast the TRNOE decays. This effect is greater for internal motions in the free peptide than it is for internal motions in the bound peptide.

While it is clear that the incorporation of internal motion within a proton pair affects the magnitude of the observed TRNOE and thus the apparent interproton distance, it is also clear that the incorporation of internal motion in a reference proton pair will affect the apparent interproton distances of all proton pairs which are calculated from the reference proton pair. This is because the TRNOE build-up behaviour of the reference pair is also dampened and 'spread-out' by the incorporation of internal motion. The effects of motion in the reference proton pair will generally compensate for the effects of motion in the observed proton pair. This occurs if the magnitudes of both the reference TRNOE and the observed TRNOE in the presence of internal motion are diminished with respect to their magnitudes in the absence of internal motion. However, the behaviour of the apparent distance calculated for a proton pair of interest as a function of mixing time is a complicated interplay of both the kinetics of relaxation of the proton pair of interest and of the reference proton pair, and so is not easily predicted.

It is clear that the more fully one takes into account internal motions within the molecule, the more closely do the apparent distances approximate the calculated average distances, and the smaller the dependence of the calculated apparent distance on the mixing time of the experiment or the fraction of bound protein. The apparent distances calculated for the intraresidue Val^{114}-αCH–$(\gamma CH_3)_2$ interaction were most accurate when a model incorporating methyl group rotation was adopted. The apparent distances calculated for the interresidue $Phe^{106}(\varepsilon CH_2\zeta CH)$–$Val^{114}(\gamma CH_3)_2$ interaction were most accurate when a model incorporating *both* methyl group rotation and ring rotation was adopted. Thus, a *full* consideration of internal motions in a molecule does increase the accuracy of the calculated distances from the observed TRNOEs.

The issues of internal motions and equivalent protons and their effects on the development of the TRNOE have been addressed in advance of a full iterative relaxation matrix approach (Boelens et al., 1989) which we will use to refine the structure of the inhibitory TnI peptide bound to TnC (Campbell and Sykes, 1989,1991b). The development of a 'TRansferred' iterative relaxation matrix approach which includes methods for calculating the effects of internal motions would be useful for refining the structures of bound ligands where mobile side chains are most certainly involved in the binding interface.

ACKNOWLEDGEMENTS

This work was supported by the Medical Research Foundation Council of Canada and the Alberta Heritage Foundation for Medical Research. The authors would like to thank Robert Boyko for writing the transferred nuclear Overhauser effect computer programs.

REFERENCES

Abragam, A. (1961) *The Principles of Nuclear Magnetism*, Oxford University Press, Oxford.
Andersen, N.H., Eaton, H.L. and Nguyen, K.T. (1987) *Magn. Res. Chem.*, **25**, 1025–1034.
Anglister, J. and Zilber, B. (1990) *Biochemistry*, **29**, 921–928.
Anglister, J., Levy, R.H. and Scherf, T. (1989) *Biochemistry*, **28**, 3360–3365.
Balaram, P. and Bothner-By, A.A. (1972a) *J. Am. Chem. Soc.*, **94**, 4015–4017.
Balaram, P. and Bothner-By, A.A. (1972b) *J. Am. Chem. Soc.*, **94**, 4017–4018.
Baleja, J.D., Moult, J. and Sykes, B.D. (1990) *J. Magn. Reson.*, **87**, 375–384.
Banerjee, A., Levy, H.R., Levy, G.C. and Chan, W.W.C. (1985) *Biochemistry*, **24**, 1593–1598.
Bevilacqua, V.L., Thomson, D.S. and Prestegard, J.H. (1990) *Biochemistry*, **29**, 5529–5537.
Bloch, F. (1957) *Phys. Rev.*, **105**, 1206–1222.
Boelens, R., Koning, T.M.G. and Kaptein, R. (1988) *J. Mol. Struct.*, **173**, 299–311.
Boelens, R., Koning, T.M.G., van der Marel, G.A., van Boom, J.H. and Kaptein, R. (1989) *J. Magn. Reson.*, **82**, 290–308.
Borgias, B. and James, T.L. (1988) *J. Magn. Reson.*, **79**, 493–512.
Borgias, B. and James, T.L. (1989) In *Methods in Enzymology, Vol. 176, Part A*, (Eds., Oppenheimer, N.J. and James, T.L.) Academic Press, New York, pp. 169–183.
Bull, T.E. (1987) *J. Magn. Reson.*, **72**, 397–413.
Campbell, A.P. and Sykes, B.D. (1989) In *Calcium Protein Signalling* (Advances in Experimental Medicine and Biology, Vol. 255) (Ed., Hidaka, H.), Plenum Press, New York, pp. 195–204.
Campbell, A.P. and Sykes, B.D. (1991a) *J. Magn. Reson.*, **93**, 77–92.
Campbell, A.P. and Sykes, B.D. (1991b) *J. Mol. Biol.*, in press.
Campbell, A.P., Cachia, P.J. and Sykes, B.D. (1991) *J. Biochem. Cell Biol.*, in press.
Clore, G.M., Gronenborn, A.M., Carlson, G. and Meyer, E.F. (1986) *J. Mol. Biol.*, **190**, 259–267.
Ehrlich, R.S. and Colman, R.F. (1985) *Biochemistry*, **24**, 5378–5387.
Ehrlich, R.S. and Colman, R.F. (1990) *Biochemistry*, **29**, 5179–5187.
Ferrin, L.J. and Mildvan, A.S. (1985) *Biochemistry*, **24**, 6904–6913.
Glasel, J.A. (1989) *J. Mol. Biol.*, **209**, 747–761.
Glasel, J.A. and Borer, P.N. (1986) *Biochem. Biophys. Res. Commun.*, **141**, 1267–1273.
Ito, W., Nishimura, M.N., Sakato, N., Fujio, H. and Arata, Y. (1987) *J. Biochem.*, **102**, 643–649.
Keepers, J.W. and James, T.L. (1984) *J. Magn. Reson.*, **57**, 404–426.
Landy, S.B. and Rao, B.D.N. (1989) *J. Magn. Reson.*, **81**, 371–377.
Lefevre, J.F., Lane, A.N. and Jardetsky, O. (1987) *Biochemistry*, **26**, 5076–5090.
Levy, H.R., Assulin, O., Scherf, T., Levitt, M. and Anglister, J. (1989) *Biochemistry*, **28**, 7168–7175.
Lipari, G. and Szabo, A. (1982) *J. Am. Chem. Soc.*, **104**, 4546–4559.
Macura, S. and Ernst, R.R. (1980) *Mol. Phys.*, **41**, 95–117.
Marshall, A.G., Schmidt, P.G. and Sykes, B.D. (1972) *Biochemistry*, **11**, 3875–3879.
Meyer, E.F., Clore, G.M., Gronenborn, A.M. and Hansen, H.A.S. (1988) *Biochemistry*, **27**, 725–730.
Milon, A., Miyazawa, T. and Higashijima, T. (1990) *Biochemistry*, **29**, 65–75.
Ni, F., Konishi, Y., Frazier, R.B., Scheraga, H.A. and Lord, S.T. (1989a) *Biochemistry*, **28**, 3082–3094.
Ni, F., Meinwald, Y.C., Vasquez, M. and Scheraga, H.A. (1989b) *Biochemistry*, **28**, 3094–3105.
Ni, F., Konishi, Y., Bullock, C.D., Rivetna, M.N. and Scheraga, H.A. (1989c) *Biochemistry*, **28**, 3106–3119.
Ni, F., Konishi, Y. and Scheraga, H.A. (1990) *Biochemistry*, **29**, 4479–4489.
Solomon, I. (1955) *Phys. Rev.*, **99**, 559–565.
Wüthrich, K. (1986) *NMR of Proteins and Nucleic Acids*, John Wiley and Sons, New York.
Yip, P.F. (1990) *J. Magn. Res.*, **90**, 382–383.